

Through-metal magnetic field communication using a ferrite-core toroid and broadband power-line modem

Kyung-Rak Sohn[†] · Hyun-Sik Kim¹

(Received March 12, 2023 : Revised April 11, 2023 : Accepted April 26, 2023)

Abstract: In this study, we present the design and implementation of a metal wall-proximity communication system that utilizes a ferrite-core toroid and broadband power-line modem. Our simulation results, obtained using COMSOL, and communication experiments using power-line modems demonstrate the potential of magnetic core toroid for magnetic field harvesting and through-metal communication. Our proposed system achieves a bandwidth of 6 Mbps in a communication test performed on a 10-millimeter-thick steel block, and real-time data communication was successfully achieved through a video transmission using an IP camera. These results highlight the effectiveness of our system for communication through metal walls and indicate its potential for various applications such as underground communication and remote sensing in harsh environments.

Keywords: Magnetic induction, Metallic enclosed sensors, Through-metal communication, Ferrite toroid

1. Introduction

The use of wireless sensors based on the Internet of Things (IoT) technology has become increasingly popular for monitoring facility conditions and collecting environmental data in both land and underwater metal structures. However, the communication of collected data through metal walls poses significant challenges. Existing wireless communication solutions, which rely on high-frequency signals, suffer from poor penetration depth into metal and high-power absorption by eddy currents. Moreover, the process of wiring through holes drilled into walls to build internal communication networks can limit design freedom and adversely affect mechanical strength, as well as result in management problems due to electrical insulation and short circuits [1].

Ultrasound has attracted considerable attention as a wireless communication method that can be applied to metal structures. Ultrasonic waves are generated using piezoelectric transducers attached to a metal surface; thus, their energy is easily transferred to the metal wall. In [2], an acoustic modem unit called “Hull-Com”, which uses the ship’s hull or frame as an acoustic path to transmit data, was unveiled. In [3], an ultrasonic transmission system that transmits energy and data through a metal wall was introduced. This system was designed to operate at a carrier frequency of 3 MHz, and the experimental results revealed that the

system achieved increased robustness against structural noise generated inside the aircraft and significantly reduced the size of the transmission system. In [4], the authors presented a technique used to significantly improve throughput in a high-speed ultrasonic communication system through a wall consisting of seven parallel channels with a bandwidth of 4.28 MHz per channel. They reported that using the measured channel data and combining the MIMO-OFDM approach with a crosstalk mitigation technique, the capacity performance reached 700 Mbps at a high-average SNR level.

Sound waves, unlike electromagnetic waves, must transmit mechanical vibrations directly to the metal; therefore, the transducer must be in contact with the metal surface. Another method is magnetic inductive coupling, which does not rely on metal-surface contact. Magnetic fields can penetrate low-permeability metals, such as iron, aluminum, and titanium, in a frequency-dependent manner.

In [5], the principle and performance of magnetic induction (MI) communication system were presented in terms of the efficiency of transmitter and receiver topologies. At frequencies below 1.4 MHz, the performance of the series-serial and series-parallel topologies is almost identical, but at high frequencies above 1.4 MHz, the series-parallel (transmitter-receiver) topology

[†] Corresponding Author (ORCID: <http://orcid.org/0000-0001-8888-1241>): Professor, Division of Electronics and Communications Engineering, Korea Maritime & Ocean University, 727, Taejong-ro, Yeongdo-gu, Busan 49112, Korea, E-mail: krsohn@kmou.ac.kr, Tel: +82-51-410-4312

¹ CEO, Matttron Co., Ltd., E-mail: hskim@matttron.kr, Tel: +82-55-232-5941

This is an Open Access article distributed under the terms of the Creative Commons Attribution Non-Commercial License (<http://creativecommons.org/licenses/by-nc/3.0>), which permits unrestricted non-commercial use, distribution, and reproduction in any medium, provided the original work is properly cited.

provides a more induced voltage to the receiver. In [6], a ferrite material was added to the transducer design for MI-based underwater radio communication for autonomous underwater vehicles (AUVs) to overcome the metal shielding effect of the hull and improve the magnetic induction signal strength. Overall, higher ferrite permeability results were obtained in a stronger magnetic field. An antenna gain of more than 18 dB can be expected if ferrite materials with relative permeability of more than 100 are applied. In [7], the first research results were presented, showing power and data transmission through aluminum using a small coil with dimensions of 15 mm × 13 mm × 6 mm. In a communication test using a 1-millimeter-thick aluminum plate, a data rate of 100 bps was obtained at a carrier frequency of 2 kHz. The results showed a BER 1×10^{-6} for the wireless power-transmission data link through aluminum. In [8], a theoretical channel model for through-metal communication in low-frequency bands was developed to predict wireless communication performance, and a 100 bps communication data rate with a centimeter-sized coil and 1 kHz carrier frequency was reported. Reference [9] reported that MI communication is a reliable and flexible solution for robot control in metal-constrained environments and that the optimal carrier frequency for a 10-millimeter-thick metal is in the low-kHz frequency band.

Transceivers used for through-metal communication have an air-core toroid or a circular coil. This is effective for power transmission achieved through a metal wall in a low-frequency region of several hundred hertz or less, but it has a bandwidth limit for high-speed data transmission. When a magnetic field is distributed around the magnetic material, the magnetic flux is concentrated in the direction of the magnetic core. Applying this to the magnetic-core toroid can increase the bandwidth of magnetic field communication.

In this study, a through-metal MI communication system was designed using a ferrite core toroid as a transceiver, connected to a broadband power line modem. COMSOL was used to model the transceiver and analyze the magnetic field distribution under metal wall conditions, with the magnetic flux density distribution visualized to compare relative attenuation as a function of carrier frequency. Communication bandwidth measurements and data communication verification were performed on a 10-millimeter-thick steel block. Overall, the study presents a novel approach to through-metal communication that has the potential to address current challenges and limitations in wireless communication solutions for metal structures.

2. Analytical Model

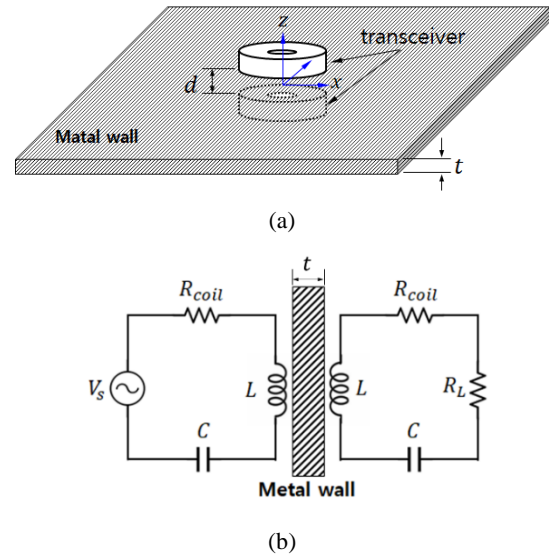


Figure 1: Configuration of through-metal MI communication. (a) Basic diagram and (b) electrical equivalent circuit

Figure 1 shows the basic model and equivalent circuit of metal-wall MI communication. The two toroids are separated by distance d , as shown in **Figure 1 (a)**, and a wide metal wall of thickness t is placed between them. The toroid facing the metal wall is equivalent to an RLC series circuit, as shown in **Figure 1 (b)**, where L denotes the self-inductance of the coil, C denotes the resonance capacitor, and R_L denotes the load resistance of the output terminal. R_{coil} denotes the coil resistance considering the AC resistance component at high frequencies, and is given by **Equation (1)**.

$$R_{coil} = \frac{aN}{r_w} \sqrt{\frac{\pi\mu f_0}{\sigma_w}}, \quad (1)$$

where a denotes the radius of the coil and N denotes the number of turns in the coil. r_w , σ_w , and μ denote the radius, conductivity, and permeability of the copper wire, respectively.

At very low frequencies, the reflection coefficients of the metals are almost negligible. However, as the frequency increases to the kilohertz region, the mutual inductance between the two magnetically coupled toroids is given as a complex number, as shown in **Equation (2)**, because the transmission and reflection coefficients are considered simultaneously [8]:

$$M = \frac{6A^2\sqrt{\mu}e^{-(1-j)t\sqrt{\pi\mu f_0\sigma_m}}}{(1-j)\pi\sqrt{\pi f_0\sigma_m}|d|^4}, \quad (2)$$

where A denotes the cross-sectional area of the coil, and σ_m denotes the conductivity of the metal. By taking the natural logarithm of both sides of **Equation (2)**, the absolute value of the mutual inductance can be obtained, as shown in **Equation (3)**.

$$\ln|M| = 2 \ln(6A) + 0.5 \ln(\mu) - \ln(\pi\sqrt{2\pi f_0 \sigma_m}) - 4 \ln(d) - t\sqrt{\pi\mu f_0 \sigma_m} \quad (3)$$

In **Equation (3)**, the mutual inductance depends on the carrier frequency and metal wall conditions. Because high-frequency signals have a relatively small skin depth compared with low-frequency signals, the magnetic field experiences a significant phase shift as it penetrates the metal. This was manifested as a shift in the resonant frequency. The high conductivity of the metal also reduces mutual inductance.

When current I is applied to the transmitter, the maximum power is delivered to the load under the condition that load resistance R_L matches coil resistance R_{coil} . The received power is expressed by **Equation (4)**. The received power is a function of carrier frequency and mutual inductance.

$$P_r = \frac{|\pi f_0 M I|^2}{2R_{coil}} \quad (4)$$

3. Numerical analysis

The geometric model built in COMSOL Multiphysics for the finite element analysis is shown in **Figure 2**. To avoid boundary reflection in the simulation space, the outer layer was set to an infinite-element domain. The metal walls also extend to match the outer layer.

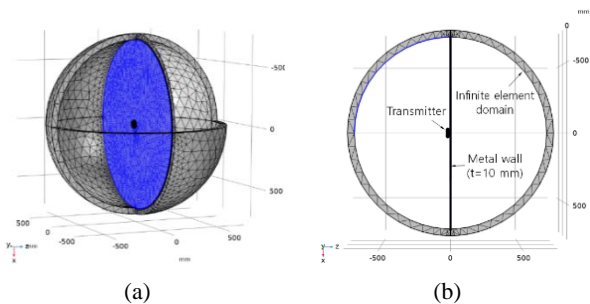


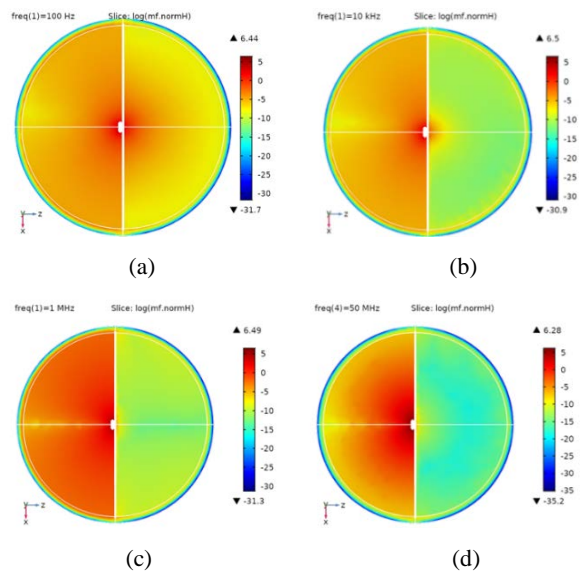
Figure 2: Simulation model ((a) 3D illustration and (b) side view)

The transducer was modeled in a toroidal shape, in which the copper wire was wound 25 times around the ferrite core with an outer diameter of 60 mm, and it was located 5 mm from the wall along the z axis. The copper wire had a radius of 0.5 mm and conductivity of 5.998×10^7 S/m. For the metal wall, nickel-

chromium-molybdenum alloy steel (AISI 4340) was selected, and its thickness and conductivity were 10 mm and 4.032×10^6 S/m, respectively. The parameters used in the simulations are presented in **Table 1**.

Table 1: Parameters and values

Symbol	Value	Symbol	Value
d	20 mm	a	20 mm
N	50	f_0	100 Hz-10 MHz
r_w	0.5 mm	A	150 mm ²
h	10 mm	I	1 A



((a) 100 Hz, (b) 10 kHz, (c) 1 MHz, and (d) 10 MHz)

Figure 3: Magnetic field distribution at several carrier frequencies. Magnetic fields are displayed using a logarithmic scale ($\log(H)$)

From the simulation results, we determined the extent to which the magnetic field generated by the toroid penetrated the metal wall. The visualized magnetic field distribution is shown in **Figure 3**. A logarithmic scale function was used to better display the magnetic field strength. As shown in **Figure 3 (a)**, a magnetic field with a frequency of 100 Hz penetrates the metal wall and is widely distributed in the opposite space. When the frequency was increased to 1 kHz, the transmitted magnetic field was concentrated around the metal wall in the opposite direction, as shown in **Figure 3 (b)**. As the frequency increased to the megahertz range, the penetrating magnetic field decayed quickly to negligible levels, as shown in **Figure 3 (c)** and **(d)**. A lower carrier frequency allows the magnetic field to penetrate the metal wall more effectively, but a higher carrier frequency is required

for strong magnetic coupling. Therefore, an appropriate carrier frequency should be selected for magnetic field transmission and inductive coupling.

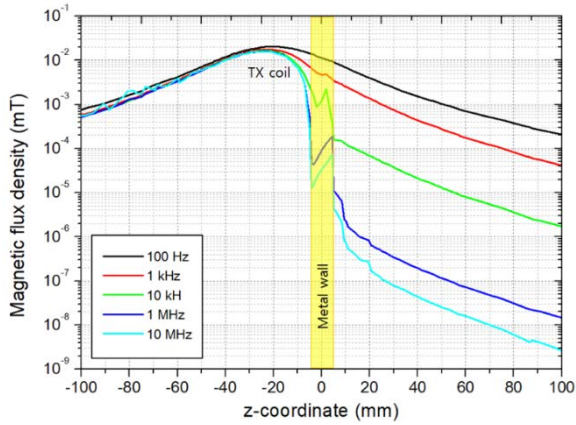


Figure 4: Magnetic flux density distribution in the z-axis direction, passing through the center of the toroid.

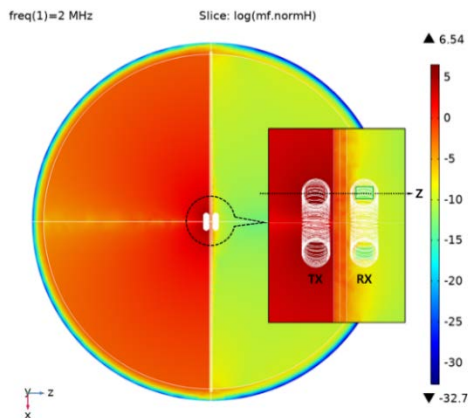


Figure 5: Magnetic field distribution with a carrier frequency of 2 MHz. The magnetic field is displayed by using a logarithmic scale, \log_{10} (H).

The flux density distribution in the z-direction, through the central axis of the toroid, is shown in **Figure 4**. At low carrier frequencies of approximately 1 kHz, the magnetic field distribution was approximately symmetrical with respect to the metal wall. At this frequency, the metal walls appeared almost transparent, allowing through-metal magnetic field communication. As the frequency increased, the magnetic field was abruptly blocked by the metal wall.

The channel bandwidth of MI communication is given as **Equation (5)** [9].

$$BW = \frac{2}{\pi^2 \gamma_w N} \sqrt{\frac{\pi f_0}{\mu \sigma_c}} \quad (5)$$

This is proportional to the square root of the carrier frequency. For high-speed data transmission, sufficient frequency bandwidth must be secured using a high-frequency carrier.

As shown in **Figure 5**, we used ferrite-inserted toroid coils to increase the radiated magnetic field in the transmitter and improve its harvesting efficiency in the receiver. The air-core coil is modeled as a magnetic dipole, where the magnetic moment is given by $m=NIA$. For a magnetic core coil, the magnetic moment multiplied by the magnetic permeability yields $m=\mu_r NIA$. The strength of the magnetic field of the receiver at distance d is given by **Equation (6)**.

$$B = \frac{\mu_0 m}{2\pi d^3} \quad (6)$$

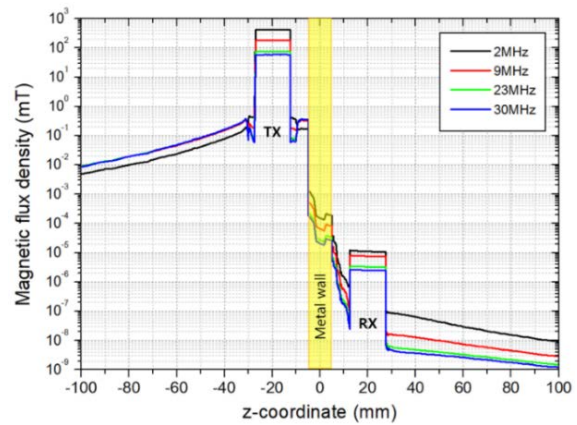


Figure 6: Distribution of magnetic flux density in the z-axis direction passing through the transmitting and receiving ferrite core

The simulation results at a current of 1 A are shown in **Figure 6**. Compared with the result shown in **Figure 4**, which is an air-core toroid, the magnetic flux density around the toroid increases by approximately 10 times. The internal magnetic flux of the transmitting toroid is 10^3 times higher than that of its surroundings. The magnetic field is rapidly attenuated by the metal wall, but the receiving toroid exhibits a magnetic flux density that is 10 times higher than that of the surrounding area. The flux energy stored in the toroid is calculated using **Equation (7)**.

$$W = \frac{B^2}{2\mu} = \frac{\mu}{8} \left(\frac{NIA}{\pi d^3} \right)^2 \quad (7)$$

As the open-circuit voltage of the receiving toroid is given by $U=2\pi f_0 BNA$, and it is controlled by the permeability of the magnetic core.

4. Experiment and results

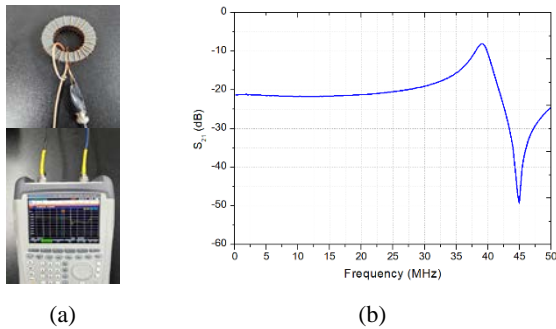


Figure 7: Ferrite-core toroid. (a) Measurement setup and (b) insertion loss, S_{21} .

Figure 7 (a) shows the toroid fabricated for the experiment. The ferrite core used a soft magnetic material synthesized with 36.16 wt% of Fe, 16.10 wt% of Cu, 13.78 wt% of Zn, and 3.22 wt% of Mg. The outer diameter of the ferrite core is 60 mm, and the number of turns is 25. The frequency response shown in **Figure 7 (b)** mainly depends on the material properties of the magnetic core. The cutoff frequency was approximately 40 MHz, and the flat-band insertion loss was approximately 20 dB.

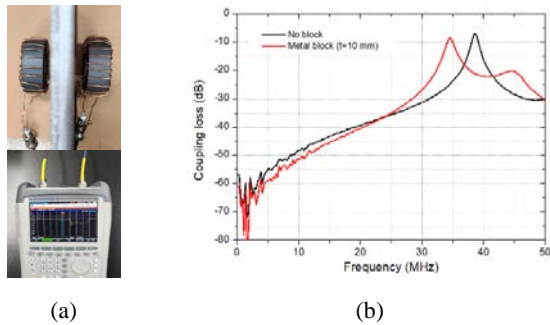


Figure 8: Signal coupling characteristic. (a) Measurement setup and (b) frequency response

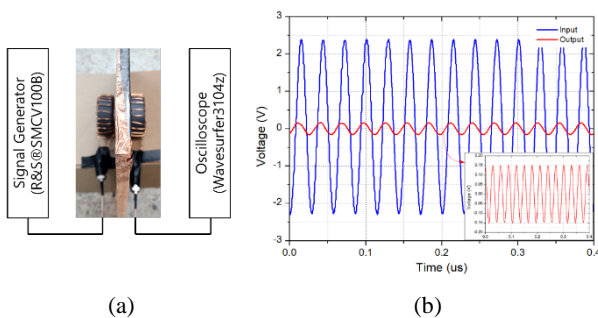


Figure 9: The output voltage of the receiver coil at resonant frequency $f_0 = 35$ MHz. (a) Measurement setup and (b) output waveform

The signal coupling characteristics between the two toroid were measured using a 10-millimeter-thick steel plate, as shown in **Figure 8 (a)**. The input-to-output signal ratio measured by the network analyzer is plotted in **Figure 8 (b)**. Strong signal coupling occurs at approximately 38 MHz when there is no metal block but switches to 35 MHz when there is a metal wall. This is because a significant phase shift occurs when an electromagnetic wave with a short wavelength passes through metal.

When a 35 MHz sine wave with a peak voltage of 2.5 V is applied to the toroid coil, the voltage induced at the output terminal is approximately 0.15 V as shown in Fig. 9. The input-to-output voltage ratio was -24 dB. At non-resonant frequencies, the signal transmission was significantly reduced. Therefore, the operating frequency band of the modem must include the toroid resonance frequency.

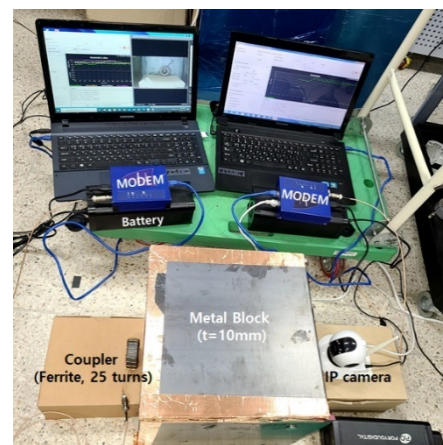
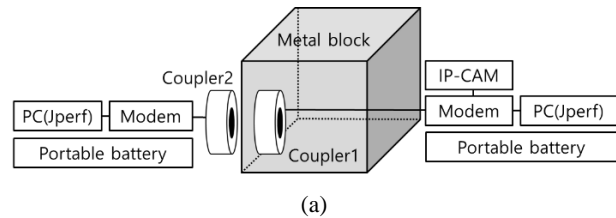


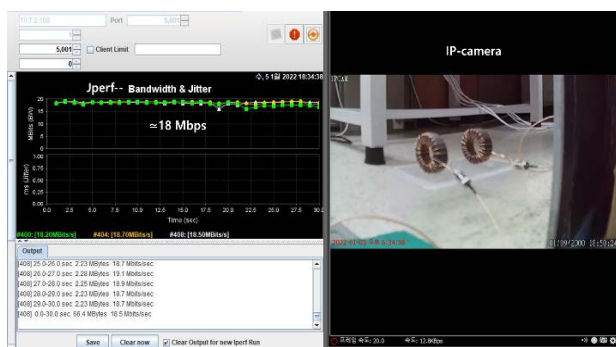
Figure 10: Experiment setup ((a) Block diagram, (b) Lab-built test bed)

A schematic of the magnetic-field communication system is shown in **Figure 10 (a)**. One toroid was installed inside the metal block, and the other was placed outside the block. The coils of the two toroids were connected to a broadband power-line communication modem (MTR-MM-D200, Matron, Korea). The modem's chipset is Intelon INT 6400 Homeplug AV, which supports data rates of up to 200 Mbps on the physical layer and operating frequencies of 2–35 MHz. A computer and an IP camera were

connected to the modem's LAN port. JPerf, a program for measuring the communication bandwidth, was used to test the connectivity, and the IP camera transmitted real-time images. Both systems were powered by independent portable batteries to prevent signal interference caused by power lines. A laboratory-built testbed is shown in **Figure 10 (b)**. The metal block consisted of five steel plates with dimensions of 300×300 (mm²) and a thickness of 10 mm. The IP camera is looking inside a metal block.



(a)



(b)

Figure 11: Bandwidth measurement ((a) On the metal block and (b) in free space)

The measurement results are shown in **Figure 11 (a)**. Despite the attenuation of the magnetic field by the metal walls, the average data rate was 6 Mbps. The IP camera captures an image of the toroid inside the metal block. The test results after removal of the metal block are shown in **Figure 11 (b)**. The IP camera image shows the toroid setup used in this experiment. The average data rate reaches 18 Mbps.

5. Conclusion

In this study, we proposed a novel through-metal communication system that utilizes a toroid and a power-line modem to overcome the electromagnetic wave blocking effect of metals. We demonstrated the flux-concentrating effect of the toroid core

through a COMSOL simulation and conducted a communication experiment on a 10-millimeter-thick metal wall using a ferrite core with copper wire wound 25 times. The results confirmed that the communication bandwidth was 6 Mbps, and successful data communication was achieved by transmitting video from an IP camera. The proposed system has the potential to be an alternative solution to communication failures caused by metal structures that are difficult to apply to existing wireless communication technologies. The use of IoT-based wireless sensors for internal monitoring of metal structures is an important application that can benefit from our proposed system. Further research is needed to optimize the system's performance and explore its potential applications in various industries.

Acknowledgment

This research was financially supported by the Ministry of SMEs and Startups (MSS), Korea, “Regional Specialized Industry Development Program (R&D, S3085628)” supervised by Korea Institute for Advancement of Technology (KIAT).

Author Contributions

Conceptualization, K. Sohn and H. Kim; Methodology, K. Sohn and H. Kim; Software, K. Sohn; Validation, K. Sohn and H. Kim; Formal Analysis, K. Sohn; Investigation, K. Sohn and H. Kim; Resources, K. Sohn and H. Kim; Data Curation, K. Sohn; Writing—Original Draft Preparation, K. Sohn; Writing—Review & Editing, K. Sohn and H. Kim; Visualization, K. Sohn; Supervision, K. Sohn; Project Administration, K. Sohn and H. Kim; Funding Acquisition, K. Sohn and H. Kim.

References

- [1] D. X. Yang, Z. Hu, H. Zhao, H. Hu, Y. Sun, and B. Hou, “Through-metal-wall power delivery and data transmission for enclosed sensors: A review,” *Sensors*, vol. 15, no. 12, pp. 31581-31605, 2015.
- [2] E. Hobart, G. Allsup, D. Hosom, and T. Baldassarre, “Acoustic modem unit,” *OCEANS 2000 MTS/IEEE Conference and Exhibition Conference Proceedings*, vol. 2, pp. 769-772, 2000.
- [3] M. Kluge, Th. Becker, J. Schalk, and T. Otterpohl, “Remote acoustic powering and data transmission for sensors inside of conductive envelopes,” *Sensors*, pp. 41-44, 2008.
- [4] J. D. Ashdown, L. Liu, G. J. Saulnier, and K. R. Wilt, “High-rate ultrasonic through-wall communications using

MIMO-OFDM,” *IEEE Transactions on Communications*, vol. 66, no. 8, pp. 3381-3393, 2018.

- [5] J. I. Agbinya, “Performance of magnetic induction communication systems using induction factors,” *Wireless Personal Communication*, vol. 70, no. 2, pp. 945-968, 2013.
- [6] D. Wei *et al.*, “Ferrite assisted geometry-conformal magnetic induction antenna and subsea communications for AUVs,” *2018 IEEE Global Communications Conference (GLOBECOM)*, pp. 1-6, 2018.
- [7] J. M. Romero-Arguello *et al.*, “Miniature coil for wireless power and data transfer through aluminum,” *Sensors*, vol. 21, no. 22, p. 7573, 2021.
- [8] H. Guo, “Through-metal wireless communications with magnetic induction,” *6th IEEE International Conference on Wireless for Space and Extreme Environments (WiSEE)*, pp. 42-47, 2018.
- [9] H. Guo and K. D. Song, “Reliable through-metal wireless communication using magnetic induction,” in *IEEE Access*, vol. 7, pp. 115428-115439, 2019.